Transition to Spatiotemporal Chaos in a Two-Dimensional Hydrodynamic System

Christophe Pirat,* Aurore Naso, Jean-Louis Meunier, Philippe Maïssa, and Christian Mathis

Institut du Non Linéaire de Nice (UMR CNRS 6618), Université de Nice Sophia Antipolis, 1361 Route des Lucioles, F-06560 Valbonne, France

(Received 24 August 2004; published 7 April 2005)

We study the transition to spatiotemporal chaos in a two-dimensional hydrodynamic experiment where liquid columns take place in the gravity induced instability of a liquid film. The film is formed below a plane grid which is used as a porous media and is continuously supplied with a controlled flow rate. This system can be either ordered (on a hexagonal structure) or disordered depending on the flow rate. We observe, for the first time in an initially structured state, a subcritical transition to spatiotemporal disorder which arises through spatiotemporal intermittency. Statistics of numbers, creations, and fusions of columns are investigated. We exhibit a critical behavior close to the directed percolation one.

DOI: 10.1103/PhysRevLett.94.134502 PACS numbers: 47.52.+j, 47.20.Dr, 68.15.+e, 68.18.Jk

Much effort has been devoted during the last two decades to the investigation of the appearance of disorder and of unpredictability in spatially extended systems. In particular, transition from a laminar to a chaotic state via *spatiotemporal intermittency* (STI) [1] was observed both numerically (coupled map lattices [2,3], partial differential equations [4,5]) and experimentally [6–8] in many one-dimensional systems. In two-dimensional (2D) systems transition to chaos via STI starting from some spatially homogeneous laminar states has been studied [9,10]. In 1986, Pomeau proposed [11] that the mechanism of STI could be analogous to directed percolation (DP), a stochastic model of contamination processes which predicts that the fraction of turbulent domains (F_t) evolves as a function of the distance from threshold ε according to a power law ε^{β}. In this Letter, we study the transition to chaos via STI in a 2D system whose laminar state is a hexagonal lattice of columns of fluid and whose turbulent state is characterized by creations and fusions of columns. Coexistence of laminar and turbulent areas, fluctuating stochastically in space and time, is clearly seen in the direct observation of the system. We propose here to study tracers closely related to the system evolution, such as the number of columns and their creation and fusion rates. These latter tracers enable us to estimate F_t.

We report experimental results on the laminar-turbulent transition concerning the dynamics of liquid columns under an horizontal porous plane which is continuously supplied. We track all columns in the grid plane and measure their number, as well as their creations and fusions induced by the dynamics. As in one dimension [12], the system is dynamically characterized by two distinct states: a laminar one and one that exhibits an intrinsic and self-organized disorder. However, the situation is different since the turbulent state appears in our system via STI instead of defect-mediated turbulence [13], a mechanism in which one does not observe coexistence of laminar and turbulent patches. Moreover, in our case the two states do not interact without external intervention. The disordered state is much like a thermodynamical state, heated by a phase turbulencelike noise. The transition from the laminar state to the turbulent one is subcritical and exhibits the characteristic trends of a first order transition including hysteresis and bistability due to competition between coexisting laminar and disordered flows.

The experimental setup, described in [14], consists of a circular and plane steel grid which is used as a porous medium and fixed horizontally at the bottom of a cylindrical tank, filled from above. The incoming fluid produces a uniform and laminar flow through the whole grid at a constant and well controlled rate q which feeds the thin layer underneath the grid. Because of the competition between gravity and surface tension [15], the flow is characterized by a wide variety of spatiotemporal structures. For an increasing flow rate, we can observe drops, liquid columns, and sheets [16]. We focus our attention on the columns regime (see Fig. 1) observed for a viscosity $\nu \gtrsim 40$ cS. It was shown in [14] that a laminar state, characterized by a stationary hexagonal organization with a wavelength λ and induced by a Rayleigh-Taylor (RT) instability with flux, generally exists in a given range of flow rates for each viscosity. At higher values of the driving force, the loss of spatial order associated to a chaotic evolution of the columns positions can be observed.

The flow surface is 200 cm^2 under the grid of thickness 1 mm with circular holes of 1 mm in diameter arranged on a 2 mm regular hexagonal lattice. We have used silicone oil with a viscosity $\nu = 50$ and 100 cS, a density $\rho = 0.97\ \mathrm{g/cm^3}$ and a surface tension $\gamma = 21\ \mathrm{dyn\,cm^{-1}}$. We present here the results obtained for $\nu = 50$ cS only, but we got qualitatively the same results for a 100 cS viscosity oil. A peripheral lighting allows us to see, from above through the grid, the local variation of the film curvature,

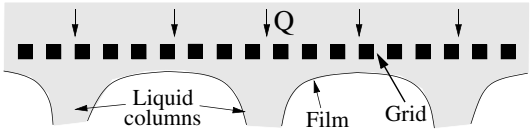

FIG. 1. Schematic drawing of the flow.

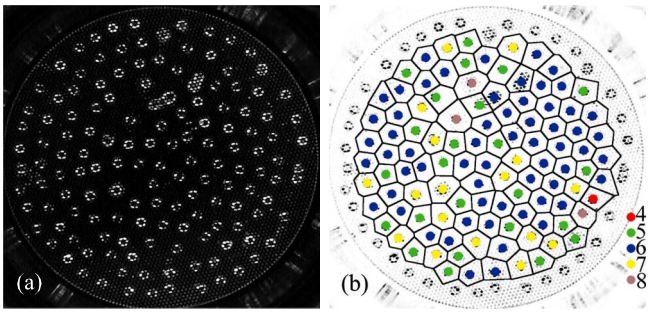

FIG. 2 (color online). (a) A typical frame and (b) its superimposed Voronoi construction. The legend indicates the number of nearest neighbors for each object.

by using the refractive properties of the oil. Liquid columns appear as small bright rings (the objects) [see Fig. 2(a)]. These objects are recorded as time frames at 25 frames/s with a digital CCD camera connected to a computer for video capture and processing. Data were recorded in 32 min long sequences for each flow rate (48 000 pictures, about 7×10^6 objects detected). An *ad hoc* image processing allows us to make an individual detection of the objects, hence to count them and to record their positions for each frame. The results are obtained by treating the data collected for seven flow rates.

The spatiotemporal chaotic state is characterized by a varying number N of columns, all of which have the same size (except in a brief transient during creation and fusion). According to the local instantaneous density of these objects, one can observe a fusion event when two columns meet, combine, and become a single one, or a creation one in a temporary low density area [see Fig. 2(a)]. These two processes both take place all the time, whereas the number of columns fluctuates around a mean value for a given flow (i.e., fixed flow rate). At low flow rate, the system is in the laminar state and $N = N_{\text{lam}}$ ($=169$ in our experiment). We find a critical flow rate $q_c = 31 \pm 2$ cm^3/s such that this laminar state is stable with respect to external finite size amplitude perturbations if $q < q_c$ and unstable if $q > q_c$, but we have experimental evidence that it is linearly stable in a range of q values. Hence the transition from the laminar to the disordered state appears to be of first order. In the following, we will use the control parameter $\varepsilon = \frac{q-q_c}{q_c}$ and the reduced number N/N_{lam} of liquid columns. We consider the situation where $\varepsilon > 0$ when the system has left the laminar regime. For increasing ε, the disorder progressively grows using the STI mechanism, the system becoming entirely turbulent for $\varepsilon > \varepsilon_2$ [see Fig. 3(a)]. For $0 < \varepsilon < \varepsilon_1$, the system exhibits bistability between STI [Fig. 3(b)] and a quasilaminar state for which the bulk is stationary and hexagonal and the peripheral columns erratically slide on the boundary, with creations and coalescences mechanisms. This quasilaminar state is due to a competition between the hexagonal order and the geometrical constraint of the circular boundaries.

In order to characterize quantitatively the transition, we first study the statistics of the number N of columns of the system. As a first step, we represent in Fig. 4 the distributions of N/N_{lam} for different values of ε. The bimodal distributions in Figs. 4(b) and 4(c) illustrate the bistability between the quasilaminar state (small peak, large values of N) and the more disordered one (large peak, small values of N). It is also interesting to note that the mean number of objects clearly decreases with increasing ε, and that N is always lower than N_{lam}. The hexagonal organization with a wavelength λ enables the most compact arrangement of the liquid columns allowed in the system. This leads us to assume the existence of a constraint of minimal distance between the objects. We calculate the distribution of the distances between nearest neighbors. It is first necessary to compute the Voronoi construction [17] of the system of columns [see Fig. 2(b)]. In this approach, each nonperipheral liquid column is located in the center of each Voronoi cell. Distributions of distances between nearest neighbors near threshold and in the disordered state are represented in Fig. 5. Independently of the value of ε, almost no pair of columns approaches nearer than 9 mm, whereas very few nearest neighbors are mutually moved away for more than 22 mm. The maximum of probability of their distances is always about 11.5 mm, which is compatible with the wavelength of the perfect hexagonal lattice of columns $\lambda = 11.6 \pm 0.1$ mm. The dispersion of the distribution increases with ε. Thus, the hexagonal organization resulting from the competition between gravity and surface tension for null or residual flow rates (RT instability) remains subjacent to the dynamics even in the disordered

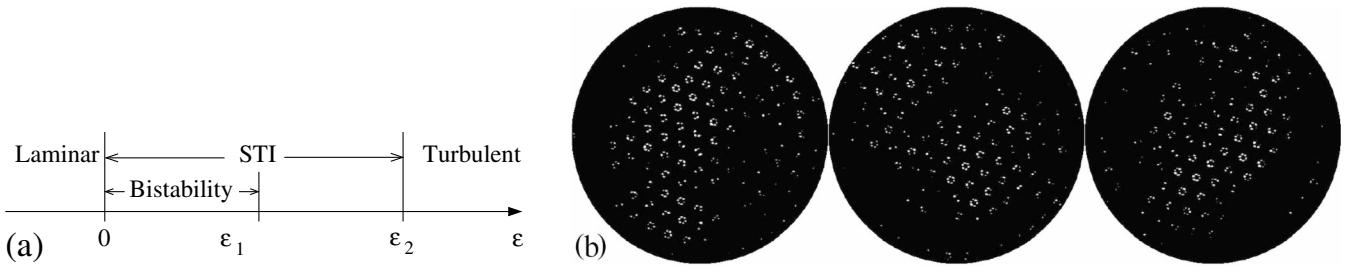

FIG. 3. (a) Schematic phase diagram for a viscosity of 50 cS as a function of the control parameter ε. (b) STI seen at three different times for $\varepsilon = 0.72$: each view is obtained through temporal average over 3 s (75 frames) to distinguish laminar areas (bright objects) from turbulent ones (dark zones).

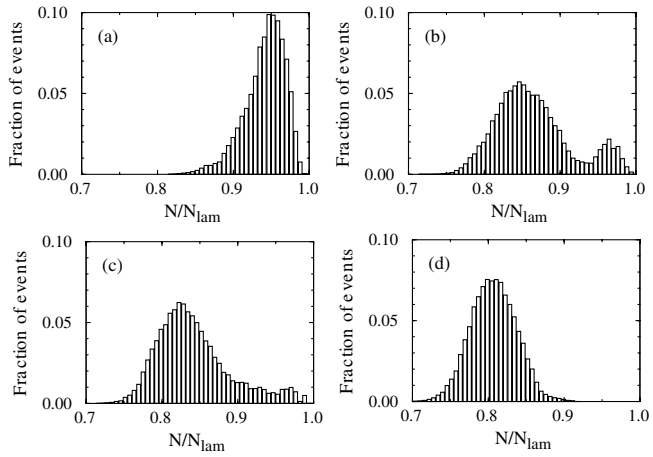

FIG. 4. Distributions of the reduced number N/N_{lam} of liquid columns for $\varepsilon =$ (a) 0.05, (b) 0.21, (c) 0.47, and (d) 0.72 ($N_{\mathrm{lam}} = 169$). For $\varepsilon \geq 0.72$, the distribution remains qualitatively similar but its average decreases with increasing ε.

state. The existence of a minimal distance between the objects can be understood by reminding that two nearby liquid columns strongly attract themselves and combine because of surface tension effects.

We choose $\langle 1 - N/N_{\mathrm{lam}} \rangle$ as an order parameter ($\langle \cdots \rangle$ denotes average over time), which enables us to plot the phase diagram of the system (see Fig. 6). In this diagram, the two metastable states are separated by distinguishing the contributions of the two peaks with $N/N_{\mathrm{lam}} = 0.93$ as a cutoff between them, respectively, for $\varepsilon = 0.21$ and $\varepsilon = 0.47$ [see Figs. 4(b) and 4(c)]. For $\varepsilon = 0.05$, it is not possible to separate both states: this regime appears as a mixture of them, the disorder coming essentially from the boundaries, with intermittent incursions (some bursts) towards the center of the system. This order parameter enables a clear determination of the bistability zone.

The N dynamics is governed by the competition between creations and fusions of the columns. This kind of behavior (perpetual creations, moves, and fusions of objects) is reminiscent of that of topological defects [18]. For this reason, we define the mean temporal creation rate in a system with N objects as $\Gamma_+(N) = \langle C_i \rangle_N$ and the fusion one as $\Gamma_-(N) = \langle F_i \rangle_N$, where C_i and F_i are, respectively,

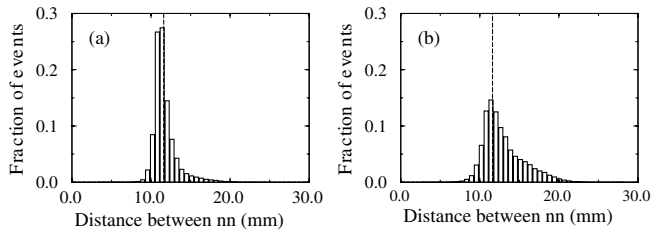

FIG. 5. Distributions of the distances between nearest neighbors for $\varepsilon =$ (a) 0.05 and (b) 0.72. The distribution evolves continuously between both states. The dashed lines indicate the wavelength measured in the stationary lattice: $\lambda = 11.6 \pm 0.1$ mm.

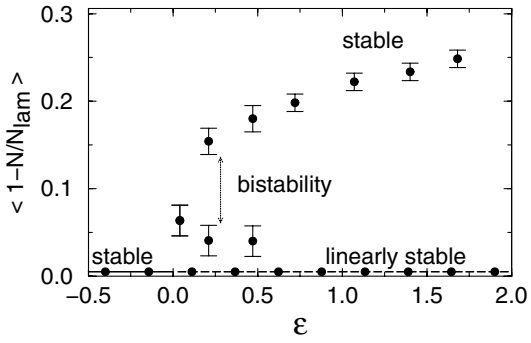

FIG. 6. Phase diagram of the system. The laminar state (line $\langle 1 - N/N_{\mathrm{lam}} \rangle = 0$) is stable for $\varepsilon \leq 0$ and linearly stable for $\varepsilon \geq 0$. After a finite size amplitude perturbation, the system leaves this state and evolves, for ε near threshold between the upper (disordered state with STI) and the lower (quasilaminar state) branch (bistability), and for higher ε on the stable upper branch where the system becomes entirely turbulent for $\varepsilon > \varepsilon_2$.

the creation and fusion numbers between frames i and $i + 1$ and $\langle \cdots \rangle_N$ denotes average over all the frames i where the number of columns N_i is N. Here, leaving and entering rates would be null because the objects can only slide on the boundaries. We present the method that we employ and our results: for each time frame, we consider each liquid column, and by comparing its position with those of the columns of the previous time frame ($\Delta t = 1/25$ s), we

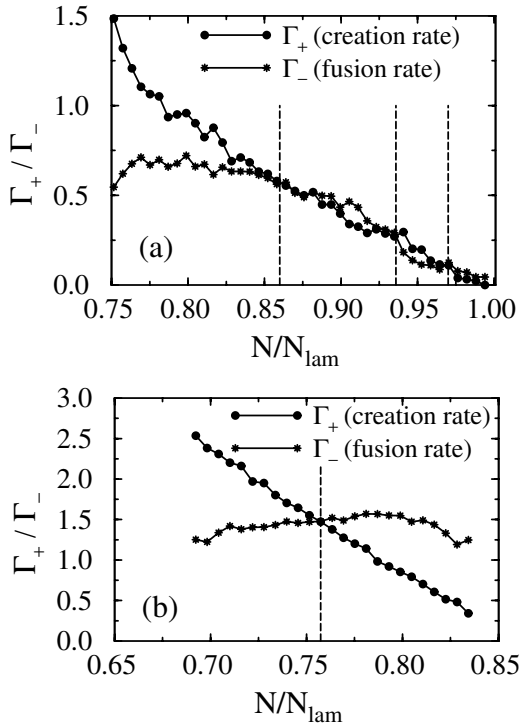

FIG. 7. Creation and fusion rates of liquid columns as a function of N/N_{lam} for $\varepsilon =$ (a) 0.21 (bistability state) and (b) 1.69 (chaotic state). The dashed lines indicate the maxima (thick lines) and the minimum (thin line) of the corresponding N distributions [see Fig. 4(b) and qualitatively Fig. 4(d)].

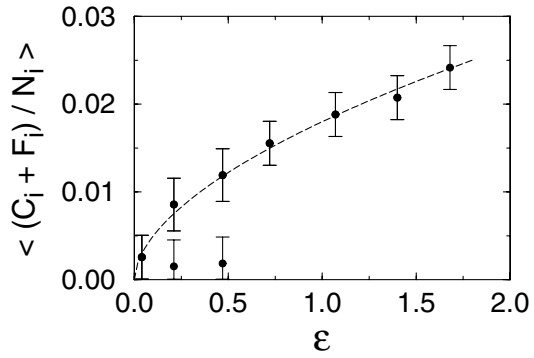

FIG. 8. Temporal average of the fraction of columns creations and fusions as a function of ε.

determine whether this object is a new one (just created), the result of the fusion of two objects (leading to the decrease by one unit), or an object which has moved. The creation and fusion durations are larger than Δt (about 3 to 4 times). The criterion we choose is the following: we calculate the distances between all the objects of the previous frame and the considered one, noting $d_1 < d_2 < d_3 < \cdots$. If $d_1 > v_{\max}\Delta t$, then we suppose that the object has been just created; if $d_2 < d_{\min}$, then we suppose that the object is the result of the fusion of two other ones. The values of $v_{\max}$ and $d_{\min}$ have been determined by preliminary tests. The creation and fusion rates are shown as a function of N/N_{lam} on Fig. 7, in two different states. In the disordered state [Fig. 7(b)], the creation rate linearly decreases with N [$\Gamma_+(N) = -\alpha_c N + \beta_c$], which can be easily understood geometrically, whereas the fusion rate slightly linearly increases [$\Gamma_-(N) = \alpha_f N$], except for large values of N (in this case, the role of the boundary constraints becomes more important). The intersection between both straight lines corresponds to the maximum of the N distribution. In the bistability state [Fig. 7(a)], the creation rate has the same behavior as in the disordered state and the fusion rate characterizes first order effects, by crossing 3 times the creation one. These three points of intersection correspond to both the maxima and the minimum of the N distribution.

These creation and fusion numbers can also be associated to another measure of the disorder since they appear only in disordered regions. We have chosen to measure $\langle \frac{C_i+F_i}{N_i} \rangle$, where $\langle \cdots \rangle$ denotes temporal average, which gives the mean degree of disorder in the system. In Fig. 8 the evolution of this average as a function of ε is represented. As for $\langle 1 - N/N_{\text{lam}} \rangle$ we have distinguished the two metastable states in the bistability region. The experimental points in the upper branch can be well fitted by a power law whose exponent is equal to 0.56 ± 0.05. As a first approximation, we consider that, at least near the critical point, the density of creations/fusions is constant into agitated domains in the STI regime. As these quantities are null in the laminar regions, one can suppose that the mean size of the agitated domains is proportional to the mean number of these events. Within this hypothesis the upper branch in Fig. 8 reflects the qualitative behavior of the mean fraction of disordered domains F_t in the STI regime and the measured exponent is in good agreement with $\beta = 0.58$ obtained from a $(2 + 1)$D model of DP [19].

Thus, the transition of our system to spatiotemporal chaos has been characterized by means of two different parameters. We have demonstrated the subcritical nature of this transition and, near threshold, the presence of bistability between STI and a quasilaminar state. In the STI regime, the turbulent fraction, described in terms of creations/fusions of objects, has been shown to vary according to a power law whose exponent is close to the $(2 + 1)$D DP one. All these studies have been done for viscosities for which disorder appears by increasing the flow rate, but for other values of the viscosity disorder can only arise by decreasing it [14]. The study of this second behavior and the transition between both will be deferred to a forthcoming publication.

The authors acknowledge helpful discussions with H. Chaté, L. Gil, and A. Pumir.

*Electronic address: Christophe.Pirat@inln.cnrs.fr

[1] H. Chaté and P. Manneville, in *Turbulence: A Tentative Dictionary*, edited by P. Tabelling and O. Cardoso (Plenum Press, New York, 1995), p. 111.
[2] K. Kaneko, Prog. Theor. Phys. **74**, 1033 (1985).
[3] H. Chaté and P. Manneville, Physica (Amsterdam) **32D**, 409 (1988).
[4] H. Chaté and P. Manneville, Phys. Rev. Lett. **58**, 112 (1987).
[5] L. Gil, Europhys. Lett. **48**, 156 (1999).
[6] F. Daviaud, M. Dubois, and P. Bergé, Europhys. Lett. **9**, 441 (1989).
[7] M. Rabaud, S. Michalland, and Y. Couder, Phys. Rev. Lett. **64**, 184 (1990).
[8] P. Rupp, R. Richter, and I. Rehberg, Phys. Rev. E **67**, 036209 (2003).
[9] H. Chaté and P. Manneville, Europhys. Lett. **6**, 591 (1988).
[10] S. Bottin, F. Daviaud, P. Manneville, and O. Dauchot, Europhys. Lett. **43**, 171 (1998).
[11] Y. Pomeau, Physica (Amsterdam) **23D**, 3 (1986).
[12] P. Brunet and L. Limat, Phys. Rev. E **70**, 046207 (2004).
[13] P. Coullet, L. Gil, and J. Lega, Phys. Rev. Lett. **62**, 1619 (1989).
[14] C. Pirat, C. Mathis, P. Maïssa, and L. Gil, Phys. Rev. Lett. **92**, 104501 (2004).
[15] D. Sharp, Physica (Amsterdam) **12D**, 3 (1984).
[16] http://www.inln.cnrs.fr/~pirat
[17] M. de Berg, M. van Kreveld, M. Overmars, and O. Schwarzkopf, *Computational Geometry: Algorithms and Applications* (Springer-Verlag, Berlin, 1997).
[18] L. Gil, J. Lega, and J. L. Meunier, Phys. Rev. A **41**, 1138 (1990).
[19] H. Hinrichsen, Adv. Phys. **49**, 815 (2000).